Available online at www.sciencedirect.com
SCIENCE DIRECT
ELSEVIER
Polymer 46 (2005) 4440–4446
polymer
www.elsevier.com/locate/polymer

Three-dimensional nano-structure of in situ silica in natural rubber as revealed by 3D-TEM/electron tomography

Shinzo Kohjiya[a], Astushi Katoh[b], Junichi Shimanuki[b], Toshinori Hasegawa[b], Yuko Ikeda[c,*]

[a]*Institute for Chemical Research, Kyoto University, Uji, Kyoto 611-0011, Japan*
[b]*NISSAN ARC, LTD., 1 Natsushima-cho, Yokosuka, Kanagawa 237-0061, Japan*
[c]*Kyoto Institute of Technology, Faculty of Engineering and Design, Matsugasaki, Sakyo, Kyoto 606-8585, Japan*

Available online 16 March 2005

Abstract

Dispersion of particulate nano-fillers has been assumed to be one of the most important determining factors of physical properties of the composites. In this paper, for the first time, a three dimensional (3D) observation of nano-structure of particulate silicas in natural rubber (NR) is reported by using a 3D transmission electron microscope (3D-TEM), which is a TEM combined with electron tomography to reconstruct 3D structural images. Here, in situ silica generated in NR matrix and a conventional silica (VN-3) mechanically mixed into NR were, without any staining of the samples, subjected to elucidation of their structural characteristics such as particle size, volume fraction and aspect ratio in NR matrix at nanometer scale. 3D-TEM/electron tomography enabled us to evaluate the density of in situ silica in NR matrix. The same samples were also subjected to atomic force microscopy (AFM) measurements to suggest a difference in the nano-filler/rubber interface area between the two samples. Since the dispersion of nano-filler in the amorphous matrix significantly controls the properties of nano-composites, 3D-TEM/electron tomography together with AFM is expected to play a most important role in revealing nanometer level 3D structure of soft materials.

Keywords: 3D-TEM; Nano-composite; In situ silica

1. Introduction

Generally, commercial rubber products are produced as composites with inorganic fillers of nanometer size, i.e. they are one kind of nano-composites. At the same time, such composites form a group of typical soft materials. In general, soft nano-composites are expanding the end uses of composite materials. Among base polymers, natural rubber (NR) has been a material of choice. Pneumatic tires for heavy-duty usages such as aircraft tires and heavy truck tires, and rubber bearings for a seismic isolation system, for example, are made from NR in conjunction with a suitable reinforcing filler system and a sulfur-cure system for crosslinking. So far, carbon black has been widely used as a reinforcer in the rubber industry. Silica, on the other hand, is rapidly increasing its utilization, especially to manufacture so-called 'Green Tires' [1,2]. Rubber/particulate-silica composites offer technical advantages over carbon black in rolling resistance and the reduction in heat build-up. A silica-filled NR is considered to be an eco-friendly, i.e. an environmentally benign 'green' material, because NR is a biomass material that is renewable, and raw materials for silica abound on the earth, while carbon black is produced from fossil oil, which is destined to depletion.

In the material design of rubbery nano-composites, the morphology of nano-fillers is a very important factor controlling the properties of the products. In case of silica, for example, the dispersion and the distribution are generally recognized to be determined by the state of aggregation and agglomeration, which are schematically shown in Fig. 1. Here, the agglomeration means a tendency to form pseudo network structures by continuous aggregation of silica particles. Unfortunately, the information on the thickness (*Z*-axis) direction of the sample can not be fully elucidated by the microscopic techniques, which may result in problematic conclusions on the state of aggregation of nano-fillers. Not only a conventional transmission electron microscopy (TEM) but also most of optical microscopies produce projected three dimensional (3D) image on a two dimensional (2D) plane.

* Corresponding author. Tel.: +81 75 724 7558; fax: +81 75 724 7580.
E-mail address: yuko@ipc.kit.ac.jp (Y. Ikeda).

0032-3861/$ - see front matter © 2005 Elsevier Ltd. All rights reserved.
doi:10.1016/j.polymer.2005.02.026

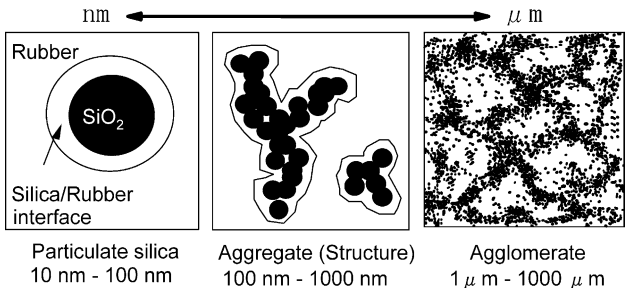

Fig. 1. Silica particle and its morphology in rubber matrix.

For 3D structural observation at nanometer scale, which is expected to afford the most accurate results, a series of (2D) TEM images at various angles is obtained by single-axis or conical tilting of a sample. 3D images are produced by backprojection of 2D TEM images using a technique of computerized tomography. The reconstruction of 3D images by these procedures is designated as 3D-TEM. With a recent development of electron tomography [3], 3D-TEM is becoming a powerful tool for the evaluation of morphology in 3D space in bioscience [3–5], and more recently in materials science [6–9] fields. The process of 3D-TEM/electron tomography used for the reconstruction of 3D nano-structure of particulate silicas in NR is presented in Fig. 2. In order to obtain accurate 3D images, 3D mass density distributions of the sample were obtained by an electron tomography technique from the backprojection of the 2D TEM images, the number of which determines the resolution. In the present study, a series of 66 2D TEM images were collected at single-axis tilt angles ranging from $-65°$ to $+65°$ in $2°$ step on a computer controlled sample stage. In 2D TEM observations, damage of the organic polymeric sample by electron irradiation limits the total possible dose and hence total number of 2D projections [3,7]. Radiation damage of the sample has been a limiting factor even in conventional (2D) TEM observations [10], which is much more enhanced in 3D-TEM. For this reason staining by a suitable reagent containing a heavy element (usually Os, Ru or U) is necessary in high-resolution TEM (and in 3D-TEM). Staining by a heavy metal is also effective for contrast enhancement.

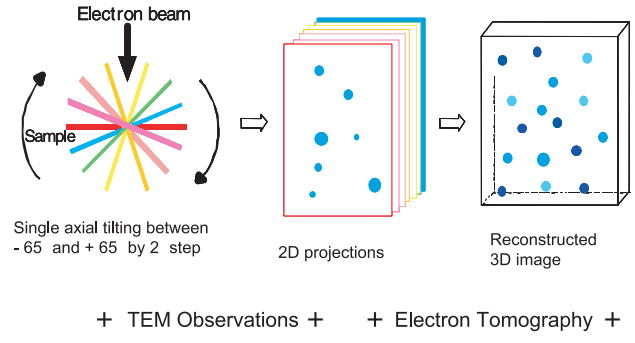

Fig. 2. 3D-TEM/electron tomography process for 3D image.

In this study, two silica-filled NR vulcanizates are subjected to 3D-TEM observation using bright-field electron tomography in order to elucidate the characteristics of in situ silica and conventional silica without staining. Different from the conventional mechanical mixing, in situ silica was directly generated in NR matrix based on the sol–gel reaction of tetraethoxysilane (TEOS), i.e. hydrolysis and condensation reactions of TEOS to produce SiO_2. In situ preparation of organic/inorganic nano-composites using the sol–gel process (a soft process) was first developed by Mark et al. for silicone elastomers [11–15] and later for diene rubbers by the present authors [16–22]. However, no 3D structural observations for these nano-composites have been reported except our preliminary communication [23]. The compounding recipes are shown in Table 1. The table includes the characteristic properties of the three compounds. Table 2 lists some physical properties of the vulcanizates including those of in situ silica-filled NR vulcanizates [20,21] some of which exceed that of conventionally filled samples: lower hardness, lower hysteresis loss, lower compression set, higher resilience, higher stress and lower storage modulus at room temperature (r.t.) were observed. In Tables 1 and 2, the NR vulcanizates without silica, with conventional silica (VN-3) and with in situ silica are abbreviated as 'NR-V', 'NR-mix-V' and 'NR-in situ-V', respectively.

In this paper, the results of atomic force microscopy (AFM) observation are presented together with those of 3D-TEM in order to investigate the states of silica surface and silica/rubber interface in the composites. Such studies are expected to be indispensable for the elucidation of structure–properties relationship in the composites based on nano-fillers. 3D-TEM observation of the conventional silica-filled NR vulcanizate is also the first one we know.

Table 1
Recipe and properties of NR mix

Sample code	NR-V	NR-mix-V	NR-in situ-V
Recipe (phr[a])			
NR	100	100	0
Stearic acid	1	1	1
ZnO	5	5	5
Sulfur	2	2	2
CBS[b]	1	1	1
Diethylene glycol	0	2	0
Commercial silica (VN-3)	0	33	0
NR with in situ silica	0	0	133
Properties of mix			
Scorch time (min)	49	>60	43
Viscosity (Pa s)	3.4×10^4	1.3×10^5	9.5×10^4

[a] Part per hundred rubbers by weight.
[b] Cyclohexylbenzothiazyl sulfenamide.

Table 2
Properties of NR vulzanizates

Sample code	NR-V	NR-mix-V	NR-in situ-V
Silica content (wt%)	0	20.1	21.4
ν[a] (mol/cm^3)	1.41×10^{-4}	7.83×10^{-5}	1.32×10^{-4}
Specific gravity	0.97	1.11	1.12
M_{50}[b] (MPa)	0.48	0.66	0.64
M_{500}[b] (MPa)	6.00	5.70	9.17
T_B[c] (MPa)	30.8	19.2	18.9
E_B[d] (%)	800	790	660
Hardness[e]	39	54	50
Compression set (%)	39	92	63
Rebound resilience (%)	82	58	67
Hysteresis behavior 1st HL[f] (%)	6.2	37.8	21.3

[a] Network-chain density measured by the micro-compression method.
[b] Stress at 50% and 500% elongations, respectively.
[c] Strength at break.
[d] Elongation at break.
[e] Shore A.
[f] HL denotes the percent of hysteresis loss relative to the stored energy.

2. Experimental

2.1. Materials

Materials and recipes for these NR vulcanizates are shown in Table 1. NR-in situ-V was prepared as follows [19,20]: a NR sheet was immersed in TEOS for 48 h at r.t. and the swollen sheet was immersed in the aqueous solution of *n*-butylamine (0.05 mol against the amount of TEOS) at 40 °C for 72 h to conduct the sol–gel reaction of TEOS. The sheet was dried under vacuum at 30 °C and was subjected to sulfur-curing at 150 °C for 20 min after mixing with curing reagents on a two-roll mill. Reference samples, NR-V and NR-mix-V, were prepared by a conventional mechanical mixing and heat pressing at 150 °C for 20 min [20]. The commercial silica used in NR-mix-V is VN-3 from Nippon Silica Co. Two parts per hundred rubber by weight (phr) of diethylene glycol was also added for NR-mix-V. The compounding recipe and some properties of these compounds are shown in Table 1, and those of the vulcanizates are shown in Table 2.

2.2. 3D-TEM/electron tomography

3D-TEM measurements were performed on a TECNAI G2 F20 (FEI Co.). The TEM imaging was carried out by the bright field method. Since both matrix NR and dispersed silicas were amorphous, the samples are not diffracting. Therefore, the bright-field electron tomography is suitable [3,7,8]. Also, high-angle annular dark-field (HAADF) imaging, using scanning transmission electron microscopy (STEM) [8,24,25], is still under a development, and its application to amorphous materials is a subject to be examined in the future.

It is noted that the NR vulcanizates were subjected in advance to the extraction by organic solvents to remove Zn compounds. The remaining Zn compounds, which were derived from ZnO (one of the additives for sulfur curing, see Table 1), scattered electron beam resulting in a smeared TEM image. The details of this effect will be published separately [26]. After this treatment, thin vulcanizate samples, whose thickness was ca 200 nm, were prepared using an ultra-microtome FC-S (REICHERT Co.) equipped with a cryo-system in liquid nitrogen. For 3D-TEM observation on the TECNAI G2 F20, 2D projection images with tilt angles ranging from $-65°$ to $+65°$ with $2°$ increment were automatically acquired at 200 kV by a CCD camera using the packaged software. The pixel size was calibrated using colloidal gold whose size was ca 10 nm as a reference. The 2D projections were aligned by using 'IMOD' [27–29]. Using a quick automatic observation system combined with a Fourier reconstruction method based on the electron tomographic technique [3,30,31], 3D mass density distributions of the samples were calculated by the backprojection of the 2D-projections, and visualized by using 'Amira' of TGS Inc. [32,33]. The data were further binarized based on the Ref. [34], after which the silica inclusions were presented as volume renderings followed by surface renderings of the reconstructed mass density distribution. In 3D-TEM photographs, the contrast was reversed in order to make the 3D images clearer. Additionally, neighboring silica particles or aggregates were displayed in different colors for easy recognition of the dispersion of silica particles.

2.3. Energy dispersion X-ray spectroscopy

The degree of removal of zinc was measured by an energy dispersive X-ray spectroscopy (EDX, ELIONIX ERA-8800 FE) using the specific X-ray intensities of Zn and Si.

2.4. Atomic force microscopy (AFM)

AFM observations were carried out using a Digital Instruments Nanoscope-III + D3100a in the tapping mode in air, where the cantilever is oscillated close to its response. Single crystal Si probes (curvature radius: 2 nm) were employed. The phase image of the response was performed by using the built-in computer software.

3. Results and discussion

Using the automatic observation system combined with a Fourier reconstruction method based on the electron tomography technique [3], 3D images of the nano-structured silicas were constructed on the TECNAI G2 F20. Fig. 3 shows one (2D-TEM) image slice for the volume rendering of the 3D reconstruction by electron tomography for NR-mix-V (a) and NR-in situ-V (b). The samples were not stained at all and without the pretreatment described in

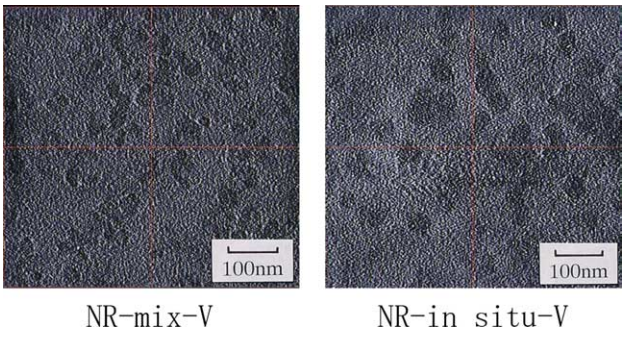

Fig. 3. One example of the sliced (2D-TEM) images of the volume rendering (a voxel projection) of 3D reconstruction by electron tomography at a *XY* plane for silica-filled NR vulcanizates before removal of zinc compounds.

the experimental section. Dark parts are identified as silica particles, but it is not easy to clearly recognize the silica particles as in reported (2D) TEM images [19–21]. For the purpose of keeping the electron beam dose as low as possible, the 3D-TEM are measured under much different conditions compared with those used in obtaining conventional 2D-TEM images. Especially, the electron beam dose was kept minimum to avoid the damage of samples. Consequently, the contrast between the rubbery matrix and the silicas is lower under the conditions for 3D structure reconstruction. This is not favorable for obtaining good 3D images. Zinc oxide in the NR vulcanizate, which was mixed with rubber for sulfur curing (Table 1), was assumed to be responsible for the low contrast, because it is generally known that the heavier is the atom the more scattered is the electron beam. Zinc oxide was reported to react with stearic acid and cure accelerators during vulcanization, and the resulting organic zinc compounds were speculated to be dissolved in the rubbery matrix [35–37]. Thus, in order to obtain a better contrast in 3D-TEM images, these zinc compounds were removed from the sulfur-cured NR by a method developed using a selective dissolution by organic solvents [26]. The quantifications of Zn and Si peak intensities by EDX on the samples before and after the extraction showed that 90% of zinc was successfully removed.

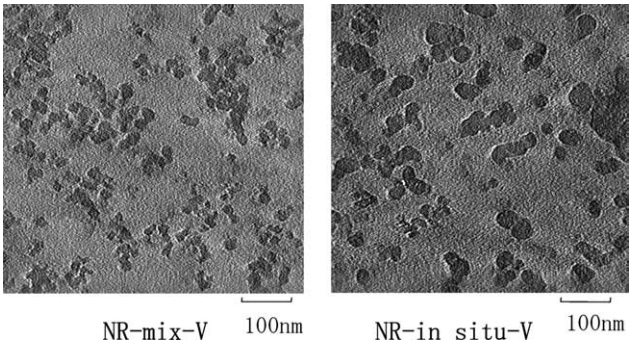

Fig. 4. One example of the sliced (2D-TEM) images of the volume rendering (a voxel projection) of 3D reconstruction by electron tomography at a *XY* plane for silica-filled NR vulcanizates after removal of zinc compounds.

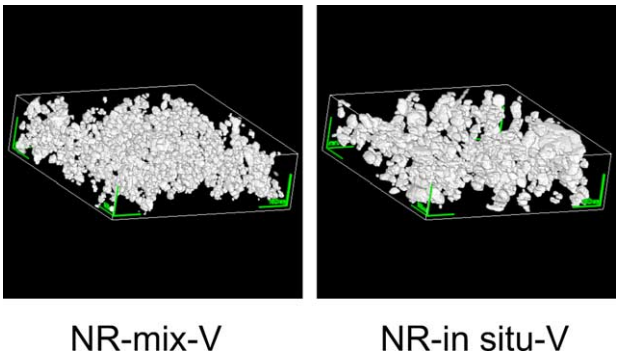

Fig. 5. Monochromic volume rendered views of the reconstructed mass density distribution of the silica inclusions for NR-mix-V and NR-in situ-V after removal of zinc compounds. The frame is shown in reconstructed perspective geometry (length and width: 630 nm, thickness: 181 nm). The green bar for each direction shows the distance of 100 nm.

As expected, better contrast was obtained as shown in Fig. 4, which displays the (2D) TEM photographs at *XY* plane of silica filled NRs after the removal of zinc atom. Comparison of Fig. 4 with Fig. 3 evidently shows the effect of removal of Zn compounds from the rubbery matrix, i.e. Fig. 4 gives much better images. It is worth noting that the effect of zinc atom observed during the 3D-TEM observations here affords the first experimental evidence of dissolution of zinc atom in the rubbery matrix in vulcanizates. This effect has been widely assumed in rubber industries, but no direct experimental results have been reported.

A series of 66 2D projections (Fig. 4 is an example) were used to reconstruct the 3D image. Fig. 5 shows the results, which are the first 3D TEM images of nano-filler in a rubbery matrix. The 3D nano-scale morphology of silicas in NR matrix is clearly visual as shown in Fig. 5, where black and white were reversed for clarity, and the white parts are identified as the silica particles. The silica is composed of a small number of primary particles and many aggregates of various sizes. It is noted that many silica particles are

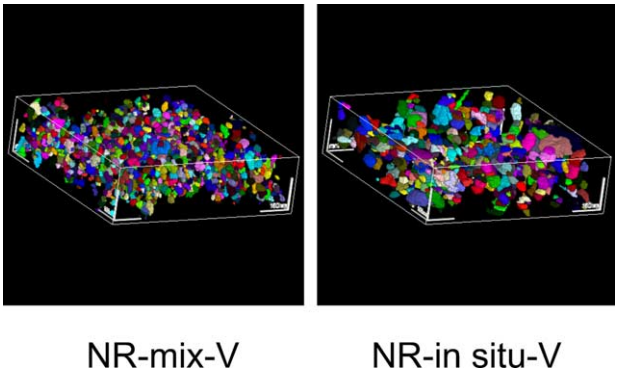

Fig. 6. Colored volume rendered views of the reconstructed mass density distribution of the silica inclusions for NR-mix-V and NR-in situ-V after removal of zinc compounds. The individual silica particles and aggregates were isolated from the neighbors by coloring. The frame is shown in reconstructed perspective geometry (length and width: 630 nm, thickness: 181 nm). The white bar for each direction shows the distance of 100 nm.

aggregated both in NR-mix-V and NR-in situ-V. For easy recognition of the dispersion of silica particles, neighboring silica particles were painted in colors, and the resulting multi-colored images are shown in Fig. 6. It must be pointed out that a colored block represents not only isolated primary silica particles but also silica aggregates. In the 3D-TEM images from various directions, many aggregates were clearly detected in both NR vulcanizates. This observation is achieved by using 3D-TEM/electron tomography for the first time. From the 3D images, the presence of agglomerates as shown in Fig. 1 was not recognized. It is suggested that the volume fraction of silica was not sufficient for percolation to occur which resulted in formation of agglomerates in NR matrix. In other words, the volume fractions, which will be described later, were lower than the percolation threshold.

3D image of the samples gives us more informations on the nano-structure of silicas in NR: The particle size of silica in NR-in situ-V is larger than that of the conventional silica (VN-3) in NR-mix-V in agreement with the results by 2D-TEM in our previous paper [19–21]. The radius, its distribution, and number of silica aggregates in a definite volume were quantitatively evaluated from this 3D-TEM/electron tomography analytical system, which are displayed in Fig. 7 with the standard deviations (SD). In situ silica was a nano-particle of average radius 13.3 nm with SD = 5.6 nm, and the size of silica in NR-in situ-V was less uniform than that of the conventional silica. The present authors (S.K. and Y.I.) have assumed that the concentration of silanol groups on the surface of in situ silica is estimated to be smaller than that of the conventional silica (VN-3) [2,20–22]. The smaller amount of silanol groups on in situ silica surface may result in a less uniform aggregation due to larger interaction with rubber molecules than that of conventional silica. However, if we consider that in situ silica was generated in the uncured NR matrix, both size and dispersion of in situ silica are still concluded to be relatively

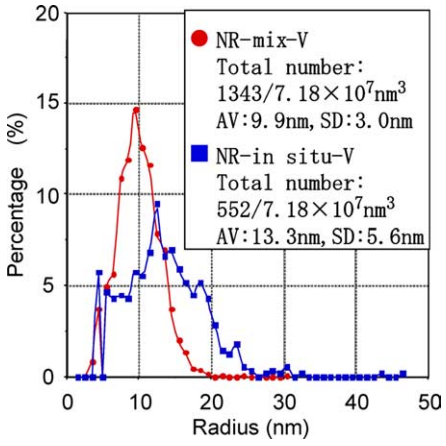

Fig. 7. Radius distribution of the conventional silica (VN-3) and in situ silica measured by 3D-TEM/electron tomography. The total number of silica in the definite volume is also displayed. ('AV' and 'SD' mean the average and standard deviation, respectively).

uniform and homogeneous, respectively. In situ silica generated in the crosslinked rubbery matrix, on the other hand, was reported to be remarkably uniform in size and very homogeneously dispersed in the matrix, probably because it was produced in a 3D chemical networks, i.e. vulcanizates [2,19]. This result was based on the conventional 2D-TEM images. They are to be subject to 3D-TEM analysis in a near future.

3D-TEM gives the volume of each particle hence the average volume of the particles and total volume of silica in the measurement volume (7.18×10^7 nm^3). The average particle volume in NR-mix-V and NR-in situ-V is 5.23×10^3 nm^3 with SD = 5.58×10^3 nm^3 and 1.41×10^4 nm^3 with SD = 1.55×10^4 nm^3. The total volume of NR-mix-V and NR-in situ-V is 7.09×10^6 nm^3 and 7.72×10^6 nm^3, respectively. Thus, their volume fractions are calculated to be 9.9% and 10.8% for VN-3 in NR-mix-V and in situ silica in NR-in situ-V, respectively. Comparison of volumes of the conventional silica (VN-3) and in situ silica enabled us to evaluate an apparent density of in situ silica in NR matrix from the specific gravity of the silica filled vulcanizates, the weight percentages of both silicas in the vulcanizates and density of the conventional silica. When the nominal value of density for VN-3 (1.95 g/cm^3) [38] was used for the calculation, the apparent density of in situ silica was found to be 1.92 g/cm^3, which was a little smaller than that of VN-3. Since the in situ silica was produced at 40 °C by the sol–gel reaction of TEOS and was dried at 30 °C under a high vacuum without further heat treatments [20–22], the slightly lower density of in situ silica is quite reasonable. In our knowledge, no results of the density of in situ silica generated in the organic matrix have been reported due to the experimental difficulty.

As one of the characteristics of the silicas, aspect ratio of the silica aggregates was calculated using the minimum length and maximum one determined in 3D-TEM images for all silica particles and aggregates. From 2D-TEM images, it is possible to calculate the aspect ratio as well as sizes of silica particles and aggregates. However, the results are much more accurate from 3D ones. The results plotted in Fig. 8 show that the in situ silica has less symmetric in shape than the conventional silica. Since in situ silica was produced and grew in the un-crosslinked NR matrix by the sol–gel reaction of TEOS, the shape of generated silica particles is liable to become non-symmetrical. Additionally, the lower concentration of silanol groups on the surface of in situ silica may give rise to less branched aggregates. For the symmetrical sphere, the primary particles may carry more silanol groups on their surface. Also, the particle size of in situ silica became larger with the increase of reaction time and catalyst concentration [39,40]. Therefore, it must be kept in mind that the detected size, shape and number of in situ silica were results on silica particles produced under specific sol–gel reaction conditions. By adjusting these conditions of the sol–gel reaction, various silicas of different sizes or characteristics may be obtained in a rubbery matrix.

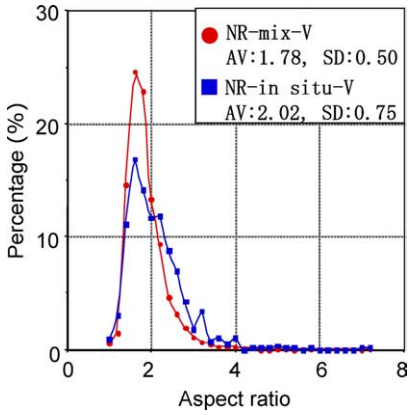

Fig. 8. Aspect ratio and its distribution of the conventional silica (VN-3) and in situ silica measured by 3D-TEM. ('AV' and 'SD' mean the average and standard deviation, respectively).

The smaller aspect ratio, i.e. less branched aggregation of in situ silica may explain the lower viscosity of the compounds (Table 1) and lower hysterisis and other physical properties of NR-in situ-V (Table 2).

In order to obtain information on interface between silica particles and NR, AFM measurements were carried out. Fig. 9 shows the results. In terms of particle sizes and dispersions, at least qualitatively similar findings are suggested by comparing Fig. 9 and Figs. 3–5. However, in the image of in situ silica in Fig. 9, the interface regions were somewhat unclear and hazy, while those of the conventional silica were relatively clear. This difference may suggest that in case of in situ silica so called immobilized rubber layer is more distinctively formed around the silica/rubber interface. The layer is supposed to be composed of strongly absorbed (sometimes described as chemisorbed) NR molecular chains due to the better wetting by NR than in the case of the conventional silica. In NR, silica-silica interaction is assumed to be much stronger than silica-rubber interaction. The chemisorbed rubber chains are supposed to form a layer around the filler surface (designated as immobilized layer [41,42]), and they adhere even in the presence of solvent. Therefore, they often called filler gels.

As stated earlier in this paper, the silanol group content

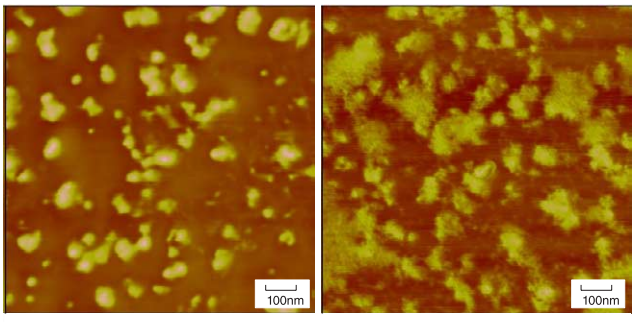

Fig. 9. High resolution AFM images of silica-filled NR vulcanizates.

on the in situ silica surface is assumed to be smaller that that on the conventional silicas. This assumption also explains the above AFM results. The smaller silanol group content on the surface of in situ silica is favorable to chemisorptions of relatively non-polar NR molecules onto the surface, which gives rise to more distinct immobilized layer (or filler gel) formation. This formation is one of the factors of better mechanical properties of NR-in situ-V than those of NR-mix-V together with the difference in aggregate morphology.

4. Concluding remarks

The 3D nanostructure of particulate silicas in NR matrix was demonstrated by 3D TEM/electron tomography technique, and a few nano-structural features of in situ silica were elucidated in comparison with the conventional silica. AFM measurements elucidated interfacial features of the particulate silicas. Silicas, including those generated in situ by the sol–gel reaction, are promising nano-fillers for the development of soft nano-composites, and the elucidation of 3D nano-structures affords important information for designing nano-composites.

Acknowledgements

The authors are grateful to Dr J. Ye, Messrs H. Sawabe, T. Suda, N. Kojima, and Ms M. Gonda and M. Nishioka (NISSAN ARK, Ltd.) for their experimental assistance and stimulating discussions. This research was partially supported by Grant-in-Aid for Science Research (B) (2) No.15404011 to S.K. from JSPS and the Research Grant from President of KIT (2004) to Y.I.

References

[1] Wolff S. Rubber Chem Technol 1996;69:325.
[2] Kohjiya S, Ikeda Y. Rubber Chem Technol 2000;73:534.
[3] Frank J, editor. Electron tomography: three-dimensional imaging with the transmission electron microscope. New York: Plenum Press; 1992.
[4] Radermacher M. J Electron Microsc Technol 1988;9:359.
[5] Koster AJ, Grimm R, Typke D, Hegrel R, Stoschek A, Walz J, et al. J Struct Biol 1997;120:276.
[6] de Jong KP, Koster AJ. Chem Phys Chem 2002;3:776.
[7] Weyland M. Top Catal 2002;21(4):175.
[8] Midgley PA, Weyland M. Ultramicroscopy 2003;96:413.
[9] Yamauchi K, Takahashi K, Hasegawa H, Iatrou H, Hadjichristidis N, Kaneko T, et al. Macromolecules 2003;36:6962.
[10] Tsuji M, Kohjiya S. Prog Polym Sci 1995;20:259.
[11] Mark JE, Pan S-J. Makromol Chem Rapid Commun 1982;3:681.
[12] Mark JE. Chemtech 1989;19:230.
[13] Mark JE. J Appl Polym Sci: Appl Polym Symp 1992;50:273.
[14] Mark JE. Heterogen Chem Rev 1996;3:307.
[15] Erman B, Mark JE. Structure and properties of rubberlike networks. London: Oxford University Press; 1997 [Chapter 16].

[16] Kohjiya S, Yajima A, Yoon JR, Ikeda Y. Nippon Gomu Kyokaishi 1994;67:859.
[17] Ikeda Y, Tanaka A, Kohjiya S. J Mater Chem 1997;7:455.
[18] Ikeda Y, Tanaka A, Kohjiya S. J Mater Chem 1997;7:1497.
[19] Ikeda Y, Kohjiya S. Polymer 1997;38:4417.
[20] Kohjiya S, Murakami K, Iio S, Tanahashi T, Ikeda Y. Rubber Chem Technol 2001;74:16.
[21] Murakami K, Iio S, Ikeda Y, Ito H, Tosaka M, Kohjiya S. J Mater Sci 2003;38:1447.
[22] Kohjiya S, Ikeda Y. J Sol–Gel Sci Technol 2003;26:495.
[23] Ikeda Y, Katoh A, Shimanuki J, Kohjiya S. Macromol Rapid Commun 2004;25:1186.
[24] Midgley PA, Weyland M, Thomas JM, Johnson BFG. Chem Commun 2002;907.
[25] Weyland M, Midgley PA, Thomas JM. J Phys Chem B 2001;105: 7882.
[26] Katoh A, Shimanuki J, Sawabe H, Suda T, Gonda M, Kojima N, et al. 7th International Conference on Nanostructured Materials, Abstract 1342, Wiesbarden, Germany, June 2004.
[27] The IMOD Home Page (http://bio3d.colorado.edu/imod/index.html), Boulder Lab. For 3D Electron Microscopy of Cells.
[28] Kremer JR, Mastronarde DN, McIntosh R. J Struct Biol 1996;116:71.
[29] Mastronarde DN. J Struct Biol 1997;120:343.
[30] Dierksen K, Typke D, Hegerl R, Koster AJ, Baumeister W. Ultramicroscopy 1992;40:71.
[31] Koster AJ, Chen H, Sedat JW, Agard DA. Ultramicroscopy 1992;46: 207.
[32] The TGS Co. Home Page (http://tgs.com).
[33] Yamamoto S, Hamada S, Nishino T, Azemoto S, Naito H, Johkoh T, et al. Nippon Hoshasen Gijutsu Gakkai-shi (J Radiol Technol, Japan) 2002;58:700.
[34] Nango N, Takeuchi K. Kinzoku (Metals, Japan) 1997;67:653.
[35] Coran AY. In: Mark JE, Erman B, Eirich FR, editors. Science and technology of rubber. 2nd ed. San Diego: Academic Press; 1994. p. 339.
[36] Krejsa MR, Koenig JL, Sullivan AB. Rubber Chem Technol 1994;67: 348.
[37] Gradwell MHS, McGill WJ. J Appl Polym Sci 1966;61:1131.
[38] Technical report on Nipsil VN-3 from Nippon Silica Co.
[39] Kajiwara K, Kameda Y, Ikeda Y, Urakawa H, Kawamura T, Urayama K, et al. Rubber Chem Technol; 2004, September/October, 2004;77:611.
[40] Ikeda Y, Kameda Y, J Sol–Gel Sci Technol, 2004;31:137.
[41] Fujimoto K. Nippon Gomu Kyokaishi 1964;37:602.
[42] Fujiwara S, Fujimoto K. Rubber Chem Technol 1971;44:1273.